Smart Structures and Systems, *Vol. 34, No. 5 (2024) 323-333*
https://doi.org/10.12989/sss.2024.34.5.323

Prediction of construction alignment for large-span bridges based on mean value theorem expansion response surface and neural network surrogate model

Xingwang Sheng [1], Xu Song [1], Weiqi Zheng*[1,2], Huanzhong Sun [1,3] and Yonghong Yang [1,4]

[1] *School of Civil Engineering, Central South University, Changsha, Hunan 410075, China*
[2] *National Engineering Research Center for High-speed Railway Construction Technology, Changsha, Hunan 410075, China*
[3] *China Railway 14th Bureau Second Engineering Co., LTD., Tai'an, Shandong, China 271000, China*
[4] *Shanghai-Hangzhou Railway Passenger Dedicated Line Co., LTD., Shanghai, China 200040, China*

(*Received August 13, 2024, Revised November 24, 2024, Accepted December 5, 2024*)

Abstract. As the span increases, the difficulty of bridge construction control continuously escalates. Accurate construction control effectively ensures that bridges maintain a reasonable stress state, proper alignment, and track smoothness. This work innovatively integrates the Mean Value Theorem Expansion Response Surface method with a Neural Network Surrogate Model to precisely identify key parameters during the construction process, achieving high-accuracy predictions of construction alignment for large-span bridges. Initially, the Response Surface-Monte Carlo method is used for the sensitivity analysis of the main construction parameters. Subsequently, a parameter identification model is established to identify and correct key parameters affecting alignment and to refine the finite element model. Based on the adjusted model, sample data are collected to create an alignment prediction network model, which predicts alignment deviations for subsequent beam segments in construction, achieving high-precision reliability assessment of bridge construction alignment. The applications of case project demonstrate that the proposed methods for structural parameter identification and alignment prediction significantly enhance the precision of alignment forecasts. Characterized by the simplicity and high accuracy of the proposed method, it can offer a novel, efficient approach for alignment control under complex construction conditions.

Keywords: alignment prediction; construction control; large-span bridge; neural network surrogate model; response surface method; sensitivity analysis

1. Introduction

Large-span bridges undergo prolonged construction and transitions in structural systems. Precise control over the construction process is essential to ensure successful closure of the spans and optimal alignment. Design parameters, often based on theoretical or standard values, can exhibit randomness due to uncertainties in construction methods and materials. Accurate construction control requires consideration of the impact of these parameters' random variability (Mia and Kameshwar 2023, Tubaldi *et al*. 2019). Given the randomness of structural design parameters, real-time error identification, state prediction, and timely adjustments are crucial to ensure the safety and functionality of the large-span bridge structure (Wang *et al*. 2023).

The variation in bridge alignment is closely associated with various construction parameters. To mitigate the impact of parameter randomness, several studies have introduced diverse approaches to enhance the precision of alignment analysis in long-span bridges. Jorquera-Lucerga *et al*. (2016) proposed a method to evaluate the effect of the ratio of main span length to side span length and the stiffness of pylons and the bridge deck. Mei *et al*. (2022) utilized uniform experimental design and multivariate stepwise regression analysis to identify key structural parameters that influence the structural response of long-span cable-stayed bridges. Shan *et al*. (2021) introduced a statistical sensitivity analysis framework designed to predict and control deviations in structural parameters during the construction of long-span cable-stayed bridges, thereby enhancing the precision of construction control. Cheng *et al*. (2019) explored the impact of structural parameters on the load-bearing performance of double-layer flat plate composite steel beams. Although existing research has extensively explored the randomness of structural parameters, current studies are still insufficient in terms of applying these insights to practical alignment control to enhance the construction precision of bridges.

Building on the consideration of parameter randomness, many studies have further concentrated on bridge alignment control. Some of these research efforts utilize computational models and optimization algorithms to enhance the accuracy and generalization capabilities of bridge construction alignment predictions (Rageh *et al*. 2019). Lu *et al*. (2021) proposed an intelligent agent model based on mind evolutionary computation-back propagation (MEC-BP) for predicting the alignment of continuous rigid frame

*Corresponding author, Ph.D., Associate Professor,
E-mail: wqzheng@csu.edu.cn

ISSN: 1738-1584 (Print), 1738-1991 (Online)

bridges during construction, effectively controlling alignment errors. Zhou *et al*. (2019) enhanced the predictive accuracy for the construction alignment of long-span continuous beam bridges by employing an optimized extreme learning machine (ELM) model. By analyzing the impact of key construction parameters and incorporating them into model training, these studies effectively manage the vast amounts of data and inherent randomness generated during the construction process, ensuring the reliability of the predictive outcomes. Other studies utilize specific data processing techniques, such as adaptive Kalman filtering and variational mode decomposition, to optimize alignment prediction tasks under construction conditions (Chen *et al*. 2016, Li *et al*. 2012). Li *et al*. (2023) took into account the randomness of influencing factors and combined the response surface-Monte Carlo method with the stochastic Kalman filter (SKF) approach to predict bridge alignment. Xin *et al*. (2022) employed an improved variational mode decomposition (IVMD) and conditional kernel density estimation (CKDE) to precisely predict bridge deformations during construction and usage, based on structural health monitoring data. However, these studies do not fully consider the randomness of construction parameters, which may limit their effectiveness in handling complex construction scenarios. Although existing research provides a multifaceted analysis of bridge alignment prediction, it often overlooks a thorough assessment of parameter sensitivity and the extent of its impact on construction. Future research needs to more deeply identify and evaluate these highly influential parameters to further optimize construction control strategies.

Artificial neural network (ANN) models are widely adopted for their nonlinear mapping capabilities. By integrating statistical analysis with numerical simulation, they accurately predict and identify changes in critical structural parameters (Saadatmorad *et al*. 2024a, b, Benaissa *et al*. 2024). Algorithms such as YUKI-RANDOM-FOREST demonstrated high precision in predicting complex structural behaviors (Seguini *et al*. 2024). In addition, neural network methods based on sparse regression provide efficient solutions for damage detection (Ghandourah *et al*. 2023). Saadatmorad *et al*. (2024c) proposed a novel damage detection method based on wavelet selection criteria, which significantly enhanced the accuracy of wavelet transform in detecting damage in metallic beam structures. ANN models showcased their capability to learn and predict the effects of multidimensional nonlinear factors, significantly improving the accuracy of structural deformation predictions and providing reliable technical support for evaluating the construction quality of large-span bridges.

In this work, the response surface-Monte Carlo method is employed to conduct sensitivity analysis on construction parameters, and then a parameter identification model is developed to identify and adjust key parameters influencing alignment. Furthermore, a neural network model is established for predicting the alignment of the main beam during the construction process. Finally, based on a case study of a large-span bridge, three parameters with the most significant impact were identified and adjusted. The neural network model was then used to predict the deformation of subsequent beam segments. This approach validated the feasibility and rationality of a large-span bridge alignment prediction method that incorporates the randomness of sensitive parameters. Therefore, the method proposed in this work can accurately identify and modify the sensitive parameters, predict deviations in the construction alignment of the subsequent beam segments, and facilitate the prediction inversion and intelligent control of the bridge alignment.

2. Sensitivity analysis for bridge cantilever construction

The randomness of construction parameters can lead to discrepancies between the measured state of a bridge structure and its theoretical design state (Jia *et al*. 2022). This work employs the mean value theorem expansion with the response surface-Monte Carlo method to perform uncertainty analysis on the construction parameters, conducting sensitivity analysis based on the statistical distribution of the construction parameters.

2.1 Establishment of response surface function

Response surface function is created by constructing explicit functions to approximate the real target function. Since the influence of each structural parameter on the target function is independent and uncorrelated (Su *et al*. 2010), and different construction parameters must be considered at each stage of construction, response surface functions are used to simulate the construction stage. Separate response surface functions are established for each independent construction stage. The expression of the response surface function is shown as Eq. (1).

$$\bar{R} = a + \sum_{i=1}^{n} b_i X_i + \sum_{i=1}^{n} c_i X_i^2 + \sum_{i=1}^{n} d_i X_i^3 + \sum_{i=1}^{n} e_i X_i^4 \quad (1)$$

Where $\bar{R}$ represents the structural response of a construction stage. $X_i (i = 1,2, \ldots . n)$ are the computational parameters that influence the structural response, and a, b_i, c_i, d_i, e_i are the coefficients to be determined.

2.2 Experimental design

In this work, ($4n$+1) sample points are selected to establish a set of equations to obtain the coefficients $a, b_i, c_i, d_i, e_i,\ (i = 1,2, \ldots . n)$ (Bucher and Bourgund 1990), and the coordinates for the experimental points are selected as shown in Table 1. By substituting the experimental sample points and their corresponding structural response results into Eq. (1), the response surface function can be solved.

2.3 Sensitivity analysis of random parameters

The random variation of construction parameters can cause stochastic changes in the response of bridge structures, and the extent of these influences can be

Table 1 Coordinates of experimental point

Experimental point coordinates	Experimental point coordinates	Experimental point coordinates
	$(\mu_{X_1} \pm \sigma_{X_1}, \mu_{X_2}, \ldots, \mu_{Xi}, \ldots, \mu_{Xn})$	$(\mu_{X_1} \pm 2\sigma_{X_1}, \mu_{X_2}, \ldots, \mu_{Xi}, \ldots, \mu_{Xn})$
	$(\mu_{X_1}, \mu_{X_2} \pm \sigma_{X2}, \ldots, \mu_{Xi}, \ldots, \mu_{Xn})$	$(\mu_{X_1}, \mu_{X_2} \pm 2\sigma_{X2}, \ldots, \mu_{Xi}, \ldots, \mu_{Xn})$
	…	…
$(\mu_{X_1}, \mu_{X_2}, \ldots, \mu_{Xi}, \ldots, \mu_{Xn})$	$(\mu_{X_1}, \mu_{X_2}, \ldots, \mu_{Xi} \pm \sigma_{Xi}, \ldots, \mu_{Xn})$	$(\mu_{X_1}, \mu_{X_2}, \ldots, \mu_{Xi} \pm 2\sigma_{Xi}, \ldots, \mu_{Xn})$
	…	…
	$(\mu_{X_1}, \mu_{X_2}, \ldots, \mu_{Xi}, \ldots, \mu_{Xn} \pm \sigma_{Xn})$	$(\mu_{X_1}, \mu_{X_2}, \ldots, \mu_{Xi}, \ldots, \mu_{Xn} \pm 2\sigma_{Xn})$

*Note: μ_{Xi} and σ_{Xi} represent the mean and standard deviation of X_i, respectively.

represented by the statistical moments of the response. For a specific construction phase, once the response surface function is obtained, take the i^{th} parameter x_i as an independent random variable, with all other parameters set to their mean values. Based on the statistical distribution of x_i, generate N samples $x_i^j (j = 1,2, \ldots N)$, this process yields N sample coordinates $(\mu x_1, \mu x_2, \ldots, x_i^j, \ldots \mu x_n)$. Substitute the N sample coordinates obtained into the corresponding response surface function and then apply the Monte Carlo method for sampling. Calculate the structural response for each sample variation and determine the standard deviation of the structural responses. When the sample N is large enough, the mean and standard deviation of the structural response R during the construction stage can be approximated, as illustrated in Eqs. (2)-(3).

$$\mu_R \approx \mu_{\bar{R}} = \frac{1}{N}\sum_{j=1}^{N} \bar{R}_j \tag{2}$$

$$\sigma_R \approx \sigma_{\bar{R}} = \sqrt{\frac{1}{N}\sum_{j=1}^{N} (\bar{R}_j - \mu_{\bar{R}})^2} \tag{3}$$

Obtaining the standard deviations of the structural responses with each parameter varies independently, so as to reflect the impact of each parameter on the structural response. The parameters with the greatest impact can be selected for parameter identification, achieving dimensionality reduction. Thus, the impact of each parameter on the structural response can be quantitatively assessed with greater accuracy. Parameters that significantly influence the structural response can be identified, providing theoretical guidance for the construction control of large-span bridges.

3. Reliability assessment for long-span bridge construction alignment

In the construction of large-span bridges, accurately identifying key construction parameters and predicting alignment requires efficient data processing and analysis (Ho *et al*. 2020). The Back Propagation (BP) neural network is a multi-layer feed forward neural network trained using the error back propagation algorithm (Yi *et al*. 2013). It effectively represents the nonlinear mapping relationships between the inputs and outputs of the neural network (Tu *et al*. 2020). In this work, considering the randomness and sensitivity of construction parameters, a BP neural network model is established to identify the main construction parameters influencing the main beam's cantilever casting alignment. This model helps obtain the

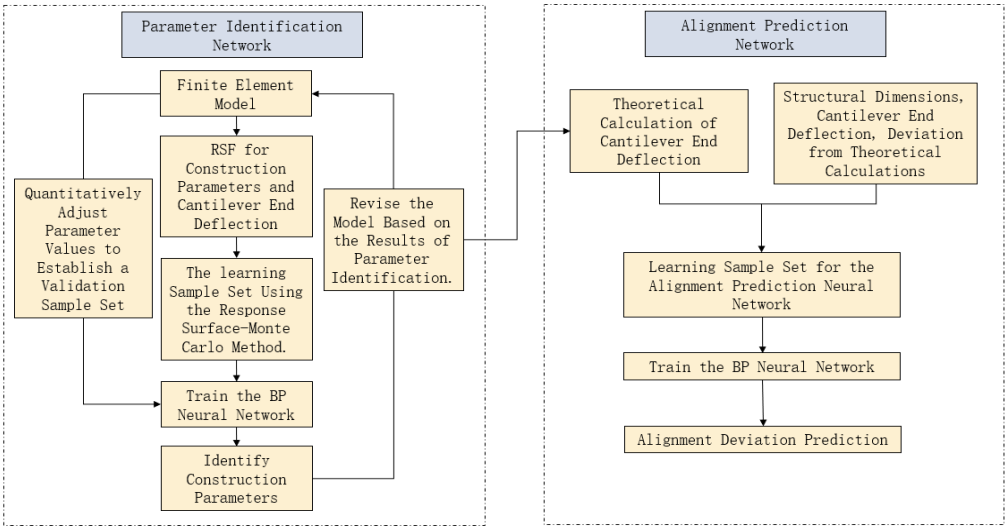

Fig. 1 Flowchart of the reliability assessment method for construction alignment of long-span bridges

actual construction parameters and refine the finite element model. Subsequently, taking into account the factors such as on-site measured data and deviations in bridge structural dimensions, a BP neural network model is established for predicting the construction alignment of the subsequent beam segments of large-span bridges. The methodological flowchart is illustrated in Fig. 1.

3.1 Identification of main beam construction parameters based on neural networks

3.1.1 Data normalization

Since the data scales of the input layer are inconsistent, it is necessary to normalize the dataset before training. Additionally, since the output range of the sigmoid-type activation functions is [0,1], extremely large or small absolute values in the dataset can lead to significant computational errors. Therefore, the range transformation method is employed to normalize the data, so as to enhance the network's learning efficiency and computational accuracy, as shown in Eq. (4).

$$X' = a + b \times \frac{X\text{-}X_{\min}}{X_{\max} - X_{\min}} \tag{4}$$

Where X represents the original data, X' is the normalized data, X_{max} and X_{min} are the maximum and minimum values of each variable group, a and b are constants determined by sample data.

3.1.2 Training strategy for the parameter identification network

In this work, the deflection at the cantilever end of the main beam is identified by focusing on the construction parameters with significantly influences. When constructing the learning set, the experimental design method is initially used to alter the construction parameters of i-th segment of the main beam for parameter identification. These parameters are then put into the finite element model to calculate the changes in the deflection at the cantilever end of the main beam. Subsequently, response surfaces are created to model the relationship between the construction parameters and each deflection difference value. Then, employing the Monte Carlo method, a sufficient number of samples are drawn and input into the response surface functions. This process yields the changes in the main beam's deflection corresponding to variations in each set of the construction parameters. The hold-out method is used to allocate 60% of the data samples, which are used as the training set, 20% of the data samples as the validation set for adjusting the model's hyperparameters, and the remaining 20% of the data samples serve as the test set to validate the model's generalization ability. Based on this, the BP neural network model is trained by the aforementioned data samples. To comprehensively evaluate the model's performance, four metrics are selected: R^2, Mean Squared Error (MSE), Mean Absolute Error (MAE), and Mean Absolute Percentage Error (MAPE). Among them, R^2 assesses the model's goodness of fit, while MSE, MAE, and MAPE reflect the errors in the training and testing datasets. After the surrogated model has been obtained, actual measurement data from subsequent beam segment constructions are collected and put into the model for parameter identification. Compare the parameter identification results with actual data, the effectiveness of the trained surrogated model can be evaluated.

3.2 Neural network-based prediction of main beam alignment

Although the identification of significant construction parameters has improved the accuracy of the finite element model, factors such as deviations in structural dimensions still cause errors in the main beam's alignment during construction. Therefore, it is necessary to predict the alignment errors of subsequent construction segments. Based on the actual conditions of bridge construction, select the factors that significantly influence bridge alignment deviations and can reflect spatial pattern characteristics serve as input parameters for the neural network surrogate model (Ye *et al*. 2022, Wang *et al*. 2018). The measured alignment deviation, ΔW, is used as the output parameter. Collect the actual measured construction deflection deviations and the dataset is also divided into training, validation, and testing sets in a 3:1:1 ratio. The model's performance is assessed using four metrics: R^2, MSE, MAE, and MAPE. After training the model, hidden layers with different numbers of layers are configured to compare the training results and determine the optimal number of hidden layers for the neural network model. Furthermore, a noise influence experiment is designed by adding Gaussian noise with standard deviations of 0.01, 0.05, and 0.1 to all input parameters. This simulates the impact of environmental disturbances and measurement errors on the model's predictive performance. The formula for noise generation is as follows

$$X_{noisy} = X_{true} + N(0, \sigma^2) \tag{5}$$

Where $N(0, \sigma^2)$ represents Gaussian noise with a mean of zero and a standard deviation of σ.

Utilize the constructed and normalized learning samples to train the BP neural network learning model, and employ the model to predict the alignment deviations of the beam ends after tensioning. Compare the predicted deflections with the actual measured deflections to evaluate the effectiveness of the main beam alignment prediction model. This comparison helps verify the model's accuracy and effectiveness in controlling the alignment of the bridge.

4. Case study

4.1 Engineering background

The Qingpu Bridge over the Taipu River, located in Qingpu District, Shanghai, is part of the Shanghai-Suzhou-Huzhou High-Speed Railway. It is a prestressed concrete continuous beam-arch combination bridge, with a span arrangement of (112+224+112) m. The layout of the bridge type is shown in Fig. 2. The main beam of the bridge is constructed using the cantilever casting method, with the mid-span beam segments labeled as 1# to 25#. After the 0#

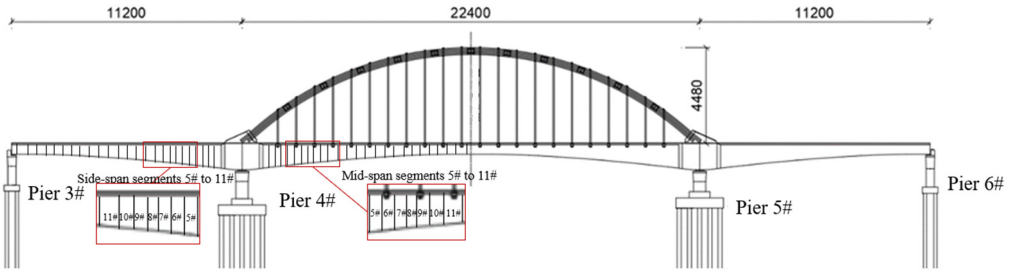

Fig. 2 The structural diagram of Qingpu Bridge (cm)

block is casted, 22 pieces of beam segments are symmetrically cantilever-cast, and the 23# and 24# blocks in the mid-span are cantilever-cast, followed by the final closure of the mid-span.

4.2 Sensitivity of main beam cantilever construction

The construction of each segment of the Qingpu Bridge includes three stages: form traveler movement, concrete casting, and prestress tensioning. During form traveler movement, adjustments to the support positions may affect the formation location and precision of the beam segments. Uneven concrete casting can lead to non-uniform settlement or deformation during curing. Improper prestress tensioning force or uneven stress distribution can affect the alignment and stability of the bridge. The prestress tensioning completion stage of the main beam's 11# segment is selected, at which point the structure is in a maximum cantilever state. The distribution types and statistical parameters of random variables during the construction of the Qingpu Bridge are detailed in Table 2 (TB 10092-2017 2017, TB 10127-2020 2020, Gong and Zhang 2022).

Employing the selected random parameters as computational variables within the above response surface function, the vertical deflection of the outermost cantilever is analyzed as the structural response. Utilizing the experimental design method described in Section 2.2, construct samples and obtain the response surface functions for each random variable varying independently, as detailed in Table 2. Conduct Monte Carlo sampling on the response surface functions for each parameter varying independently, performing 1.0×10^7 samples. Calculate the standard deviation of the structural response due to individual parameter variations as a measure of sensitivity. The results are presented in Table 3 and Fig. 3.

The greatest influence on the main beam alignment is the concrete unit weight used in the cantilever casting segments, accounting for 34.96% of the impact among all measured parameters. The main beam's concrete elastic modulus contributes 9.8% to the overall impact during this construction phase. The tensioning force of the steel strands also significantly affects the main beam alignment, collectively constituting 38.67% of the total impact. The unit weight of the current segment has a substantial impact, whereas the influence of the unit weight from previous segments can be considered negligible. The influence of the main beam's concrete elastic modulus increases with the

Table 2 Random parameters in construction stage 35

Random variable	Distribution type	Unit	Mean	Coefficient of variation	Number of random variables
Main beam elastic modulus E_C	Normal	10^4 MPa	3.6	0.05	1
Main beam segment equivalent unit weight G	Normal	kN/m^3	26	0.05	11
Steel strand tensioning force T	Normal	MPa	1260/1300	0.04	2
Form traveler weight G_g	Normal	kN	2500	0.05	1
Uniform temperature difference △t	Normal	℃	7.61	0.64	1
Relative humidity ρ	Normal	%	70	0.05	1

*Note: μ_{Xi} and σ_{Xi} represent the mean and standard deviation of X_i, respectively.

Table 3 Sensitivity of structural response to individual parameter variations

Variable name	**G1**	**G2**	**G3**	**G4**	**G5**	**G6**	**G7**	**G8**
Impact	0.07%	0.07%	0.07%	0.07%	0.09%	0.09%	0.15%	0.24%
Impact proportion	0.10%	0.10%	0.10%	0.10%	0.13%	0.13%	0.21%	0.35%
G9	**G10**	**G11**	**Ec**	**T1**	**T2**	**Gg**	**Δt**	**ρ**
0.44%	0.74%	24.16%	6.78%	18.75%	7.98%	0.44%	8.73%	0.25%
0.63%	1.06%	34.96%	9.80%	27.12%	11.55%	0.63%	12.63%	0.37%

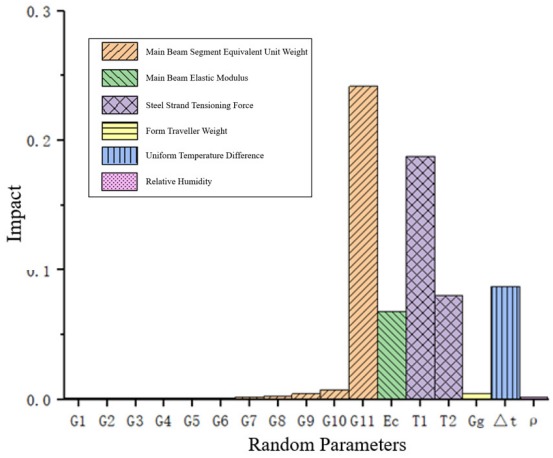

Fig. 3 The impact of random parameters during construction stage 35

extension of the cantilever. The impact of the tensioning force of the steel strands and overall temperature rise on the displacement at the cantilever end decreases as the cantilever extends. However, in the closure phase, the influence of various post-tensioning longitudinal forces becomes significant. Therefore, the tensioning force has a considerable impact and must be considered as a primary factor, while the influence of uniform temperature differences is minor and can be disregarded.

4.3 Neural network-nased parameter identification of main beam construction

Based on the analysis of the parameters' impact levels, three parameters with great influences, including concrete unit weight, elastic modulus, and tensioning force of steel strands, are allowed to vary randomly according to their distributions. The changes in the deflection at the cantilever end of the main beam resulting from these variations are calculated by the finite element model, thus generating sample data for the neural network dataset.

According to the training strategy for the parameter identification network, the input parameters are selected from the dataset samples as the deflection changes caused by casting concrete and tensioning steel strands in segments 10#, 9#, 8#, and 7# (The differences in deflection before and after casting for segments i-3#, i-2#, i-1#, i# are denoted as ΔH1, ΔH2, ΔH3 and ΔH4, respectively. Similarly, the differences in deflection before and after tensioning the prestress for segments i-3#, i-2#, i-1#, i# are denoted as ΔV1, ΔV2, ΔV3 and ΔV4, respectively). The output parameters are the three parameters for segment 10#. The input and output parameters for the parameter identification network are listed in Table 4. In the table, '*i*' represents the segment number of the beam to be identified.

Table 5 Neural network hyperparameter settings

Activation function	Hidden layer sizes	Tolerance	max iter
Relu	17	0.0001	1000

Therefore, the input layer of the parameter identification neutral network consists of 8 neurons, and there are 3 output neurons. According to Kolmogorov's theorem (Tarhouni *et al*. 2022), a 17 neurons three-layer neural network with a single hidden layer is sufficient to map all continuous nonlinear functions. The hyperparameters of the neural network are presented in Table 5. Based on the statistical patterns of the identified parameters, 1000 samples are generated by random variations. These samples are then divided into a training set, validation set, and test set at a ratio of 3:1:1. Statistical description of input features of the database including the range ([min, max]), mean, median, mode and standard deviation (STD) values of all the features is shown in Table 6.

The performance of the neural network is evaluated by Mean Squared Error (MSE), Mean Absolute Error (MAE), and Mean Absolute Percentage Error (MAPE) based on the test set. The performance of the neural network is depicted in Fig. 4. The coefficient of determination, R^2, is 0.9927, indicating a high correlation between the neural network's output data and the expected output data. The MSE, MAE, and MAPE for the concrete unit weight of the 10# segment are 0.0031%, 0.0280%, and 3.6483%, respectively. The MSE, MAE, and MAPE for the concrete elastic modulus of the 10# segment are 0.0004%, 0.1425%, and 9.7586%, respectively. For the tension force of steel strands in 10# segment, the MSE, MAE, and MAPE are 0.0019%, 0.0186%, and 2.6517%, respectively. The errors between the trained neural network output data and the expected output data are relatively similar, allowing for predicting construction parameters effectively.

Table 4 Input and output parameters for the parameter identification network

Type	Parameter Name	Type	Parameter Name
Input	ΔH1: Deflection change before and after casting of segment i-3#	Output	G: Equivalent unit weight of concrete for segment i#
	ΔH2: Deflection change before and after casting of segment i-2#		E: Elastic modulus of concrete for segment i#
	ΔH3: Deflection change before and after casting of segment i-1#		T: Prestress in steel strands for segment i#
	ΔH4: Deflection change before and after casting of segment i#		
	ΔV1: Deflection change before and after tensioning of segment i-3#		
	ΔV2: Deflection change before and after tensioning of segment i-2#		
	ΔV3: Deflection change before and after tensioning of segment i-1#		
	ΔV4: Deflection change before and after tensioning of segment i#		

Table 6 Sample subset from the parameter identification neural network dataset

Parameter name		Unit	Range	Mean	Median	Mode	STD
Casting deflection (mm)	10# Block	mm	[-2.09, -1.70]	-1.89	-1.89	-2.09	0.06
	9# Block		[-2.64, -2.14]	-2.38	-2.38	-2.60	0.07
	8# Block		[-3.28, -2.66]	-2.97	-2.97	-3.21	0.10
	7# Block		[-3.92, -3.16]	-3.53	-3.53	-3.91	0.12
Tension deflection (mm)	10# Block		[1.76,2.04]	1.91	1.91	1.86	0.03
	9# Block		[2.36, 2.73]	2.55	2.55	2.54	0.05
	8# Block		[3.20, 3.70]	3.46	3.46	3.20	0.07
	7# Block		[4.17, 4.83]	4.51	4.51	4.17	0.09

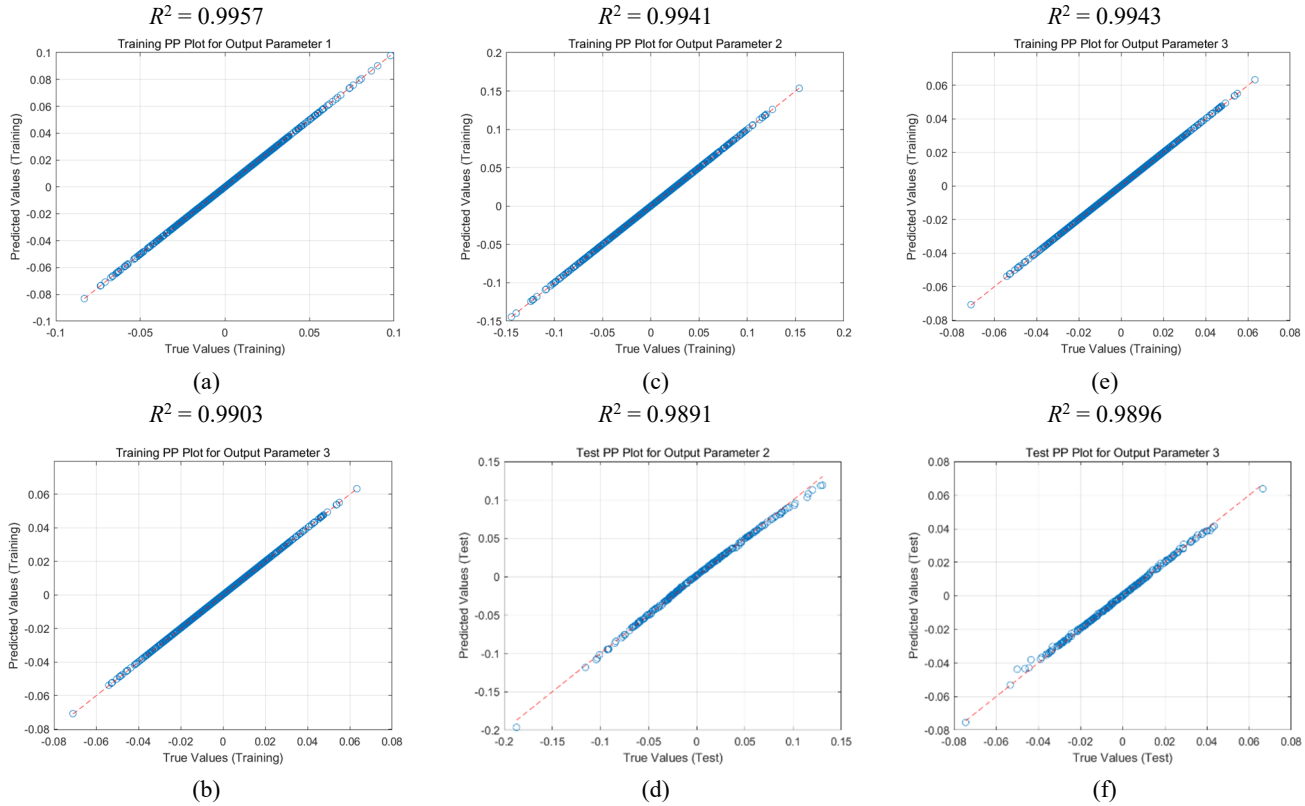

Fig. 4 Performance of the construction parameter identification network on the training set and test set

After the completion of the 10# beam segment construction, parameter identification for the concrete unit weight, elastic modulus, and steel strand tensioning force of the 10# segment is conducted using the actual measured deflection data from the cantilever ends of the 7#, 8#, 9#, and 10# beam segments, which resulted from the casting and tensioning of the 10# segment. The input vector P formed from the measured data is P = [-1.99, -2.51, -3.13, -3.72, 1.86, 2.48, 3.37, 4.37]. This vector is input into the trained neural network model, yielding the result vector T for parameter identification of the 10# segment as T = [4.68%, 17.2%, -2.64%], as shown in Fig. 5. Based on the predicted results, the adjusted concrete unit weight of is 26 × (1 + 4.68%) = 27.2 kN/m^3; the adjusted concrete elastic modulus is 3.6 × 10^4 × (1 + 17.2%) = 4.220 × 10^4 MPa; and the tensioning force of the prestressed steel strands is (1-2.64%)× σ_{con} =97.36%× σ_{con}. After the actual construction

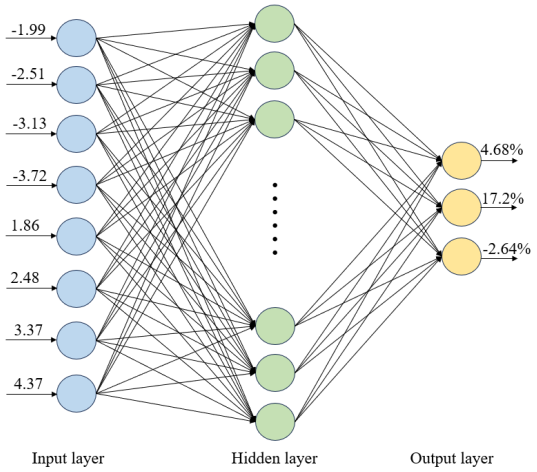

Fig. 5 Neural network parameter identification results

Table 7 Input and output parameters for the alignment prediction network

Type	Parameter name	Parameter symbol	Unit
Input	Distance from the tensioning section to the bridge pier center	*L1*	cm
Input	Distance from the section under discussion to the bridge pier center	*L2*	cm
Input	Height of the box girder at the tensioning section	*H1*	mm
Input	Height of the box girder at the section under discussion	*H2*	mm
Input	Theoretical Calculation of Elevation Change After Casting	*W1*	mm
Input	Theoretical Calculation of Elevation Change After Tensioning	*W2*	mm
Output	Measured alignment deviation	ΔW	mm

Table 8 Sample subset from the alignment prediction neural network dataset

Parameter name	Unit	Range	Mean	Median	Mode	STD
Height of the box girder at the tensioning section	cm	[2750, 4750]	4033	4300	4750	624
Height of the box girder at the section under discussion	cm	[2750, 4750]	3366	3100	2750	585
Distance from the tensioning section to the bridge pier center	mm	[840, 1040]	910	883	844	59
Distance from the section under discussion to the bridge pier center	mm	[840, 1040]	974	1000	1036	57
Theoretical Calculation of Elevation Change After Casting	mm	[-3.8, -0.3]	-1.4	-1.2	-3.8	0.9
Theoretical Calculation of Elevation Change After Tensioning	mm	[1.0, 4.5]	1.9	1.5	1.5	0.9

of segment 10#, the true values of the three construction parameters are measured and compared with the predicted values. The field-measured concrete unit weight of the main beam is 26.8 kN/m^3, the concrete elastic modulus is 4.217 × 10^4 MPa and the actual prestressing force of the steel strands is 97.59% × σ_{con}, with relative errors compared to the model's predicted values being 1.47%, 0.7‰, and 0.53%, which closely align with the values identified by the trained neural network model.

4.4 Neural network-based alignment prediction of main beam construction

In this work, the actual measured construction deflection deviations are collected as sample data for the learning and testing sets of the alignment prediction neural network. The following six parameters are used as input parameters for the neural network surrogate model: The heights of the box girder at the tensioning and discussion section, *H*1 and *H*2; The distances from the tensioning section and the section under discussion to the center of the bridge pier, *L*1 and *L*2; The calculated changes in elevation after casting and tensioning at the cantilever end of the segment being cast in this phase, *W*1 and *W*2. The measured alignment deviation, ΔW, is used as the output parameter. The input and output parameters for the alignment prediction network are as follows in Table 7.

The neural network structure of the main beam alignment prediction includes an input layer with 6 neurons, an output layer with 1 neuron, and a hidden layer consisting of 13 neurons. Predict the deviation deformation of beam segments during the construction phase following the 1/2 maximum double cantilever (Stage 11#). Gather and organize field-measured data as learning samples for the neural network. Statistical description of input features of the database including the range ([min, max]), mean, median, mode and standard deviation (STD) values of all the features is shown in Table 8. Neural networks with 1, 2, and 3 hidden layers are constructed respectively and the hyperparameters of the neural network are presented in Table 9. The performance of the neural network is depicted in Fig. 6. The comparison reveals that the model with a single hidden layer achieves the highest R^2, indicating the best fit to the data. The coefficient of determination, R^2, is 0.9773, indicating a high correlation between the output data from the neural network and the expected output data. The MSE, MAE, and MAPE for the measured elevation changes after tensioning are 0.0135 mm, 0.1034 mm, and 16.1238%, respectively.

Table 9 Neural network hyperparameter settings

Activation function	Hidden layer sizes	Tolerance	Max iter
Relu	(13)	0.0001	1000
Relu	(13,27)	0.0001	1000
Relu	(13,27,55)	0.0001	1000

To evaluate the applicability and robustness of the proposed method in actual construction scenarios, Gaussian noise with standard deviations of 0.01, 0.05, and 0.1 was added to the training dataset to simulate the effects of environmental disturbances and measurement errors on the model's predictive performance. The neural network was retrained using the noise-added training datasets, and the key performance indicators under different noise levels were analyzed. The results are presented in Table 10. As observed from the table, with the increase in noise level σ, the model's prediction error gradually rises, with MAPE increasing from 16.1238% to 35.0680%. However, the model still demonstrates good predictive performance when $\sigma \leq 0.05$.

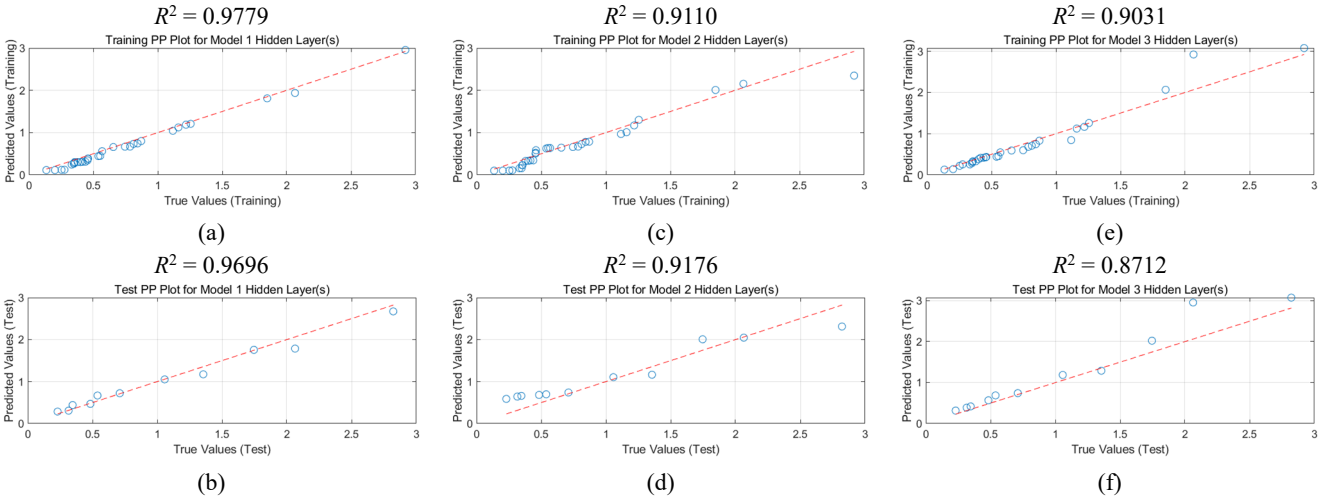

Fig. 6 Performance of the alignment prediction network on the test set

Table 10 Model predictive performance under different noise levels

Noise levels σ	R^2	MSE (mm)	MAE (mm)	MAPE
0	0.9773	0.0135	0.1034	16.1238%
0.01	0.9562	0.0260	0.1275	20.7541%
0.05	0.9528	0.0278	0.1361	21.0325%
0.1	0.5384	0.2789	0.3834	35.0680%

Using the trained neural network, predict the alignment deviations after tensioning of the side-span at Pier 4# and segment 11# of the mid-span main beam. Based on the predicted results, the forecasted elevation is calculated. Upon completion of the construction, the actual elevation is collected, and the theoretical elevation is determined using the finite element model. The three values are then compared to validate the effectiveness of the model's predictions. Some results are presented in Table 11.

From Table 8 and Figs. 7(a)-(b), it is evident that the predictions from the alignment prediction model are consistent with the observed changes in the actual measurements. The largest prediction deviation at the mid-span location is -0.75 mm, occurring at the section of the 11# beam segment, while the largest theoretical deviation is -1.78mm. The deviations between the predicted values and the actual measurements are smaller across all sections, averaging 50% of the theoretical deviations. At the side-span location, the largest prediction deviation is -0.69 mm, compared to the largest theoretical deviation of -1.71 mm,

Table 11 Deflection changes for sections 5# to 11# after tensioning of segment 11# (mm)

Construction stage	Location	Beam segment section number	Predicted deflection	Measured deflection	Theoretical deflection	Deviation between theoretical and measured	Deviation between predicted and measured
11#	4# Mid-span	5	0.61	0.291	1.074	-0.83	-0.36
		6	1.06	0.494	1.476	-0.82	-0.41
		7	1.39	0.742	1.962	-1.30	-0.73
		8	1.89	1.361	2.621	-1.26	-0.53
		9	2.82	2.110	3.507	-1.26	-0.57
		10	3.59	2.930	4.606	-1.68	-0.66
		11	4.87	4.120	5.896	-1.78	-0.75
	4# Side-span	5	0.58	0.354	1.072	-0.72	-0.23
		6	0.96	0.560	1.475	-0.92	-0.40
		7	1.29	0.750	1.960	-1.01	-0.34
		8	1.69	1.220	2.619	-1.17	-0.24
		9	2.63	2.070	3.505	-1.14	-0.26
		10	3.62	3.050	4.604	-1.65	-0.67
		11	4.88	4.184	5.894	-1.71	-0.69

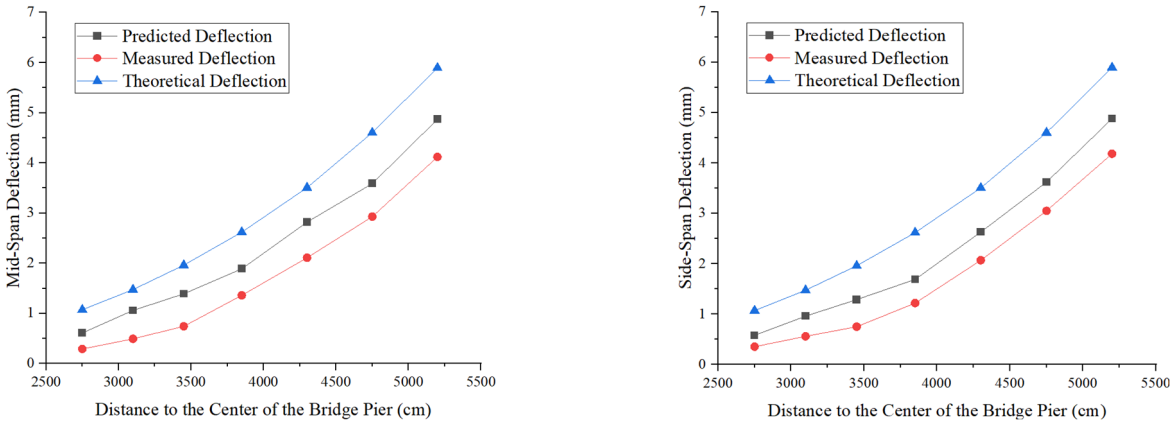

(a) Comparison of deflections at the mid-span (b) Comparison of deflections at the side-span

Fig. 7 Comparison of deflections at the mid-span and side-span of pier 4#

with the prediction deviations averaging 30% of the theoretical deviations. The above observations demonstrate that the trained alignment prediction model can effectively map the deformation patterns of bridge structures. Compared to traditional theoretical calculation models, this prediction model exhibits generally smaller prediction deviations when mapping structural deformations of bridges. By inputting parameters, it quickly provides responses with smaller deviations, offering more accurate and reliable results in the reliability assessment of bridge construction alignment.

5. Conclusions

Addressing the issue of alignment control in the construction of large-span bridges, this study conducted a sensitivity analysis of the main construction parameters, identified critical parameters for construction, and predicted alignment deviations for subsequent beam segments. The methods were applied in an actual bridge project, with the predictive results compared to measured deflections. The main conclusions are as follows:

- A sensitivity analysis method for major construction parameters based on the response surface-Monte Carlo method was proposed. Establish a construction parameter identification model to further identify and correct parameters with high sensitivity, leading to enhanced accuracy in structural prediction.
- A neural network model was developed for predicting the construction alignment of the large-span bridge. By modifying the key parameters, which has been identified, the alignment deviations in subsequent beam segments can be predicted.
- Case analysis validated the reliability and accuracy of the large-span bridge alignment prediction method based on the neural network surrogate model, demonstrating the model's practicality and efficiency in enhancing the reliability assessment of bridge construction alignment.
- This work allows for the identification and modification of significant construction parameters, enabling the alignment deviation prediction, and the alignment reliability assessment based on the trained neural network provides practical guidance for the construction control of large-span bridges.

This study has certain limitations in parameter selection, the precision of stochastic analysis, and the comprehensiveness of neural network applications. Future research could expand the parameter range, consider the correlations between parameters, and optimize model selection to enhance the accuracy of construction alignment predictions and improve the model's applicability.

Acknowledgments

This work was supported by the National Natural Science Foundation of China (NO. 52078488 and NO. 52308223), the Key Technologies for the Construction and Operation & Maintenance of 'One Bridge, One Tunnel' on the Yongzhou Railway (No. P2022G054), and the In-depth Study on Key Technologies for the Construction and Operation & Maintenance of the Hangzhou Bay Cross Sea Railway Bridge (No. N2024G043).

References

Benaissa, B., Kobayashi, M., Al Ali, M., Khatir, S. and Shimoda, M. (2024), "A novel exploration strategy for the YUKI algorithm for topology optimization with metaheuristic structural binary distribution", *Eng. Optimiz.*, 1-21. https://doi.org/10.1080/0305215X.2024.2349104

Bucher, C. and Bourgund, U.A. (1990), "A fast and efficient response surface approach for structural reliability problems", *Struct. Safety*, **7**, 57-66. https://doi.org/10.1016/0167-4730(90)90012-E

Chen, Z., Tim, K., Liu, S., Zhou, J. and Zeng, Y. (2016), "Application of a self-adaptive kalman filter approach in alignment control for an extra long span rail transit cable-stayed bridge", *Struct. Infrastr. Eng.*, **13**, 1-12. https://doi.org/10.1080/15732479.2016.1257644

Cheng, J., Xu, M. and Xu, H. (2019), "Mechanical performance analysis and parametric study of double-deck plate-truss composite steel girders of a three-tower four-span suspension

bridge", *Eng. Struct.*, **199**, 109648. https://doi.org/10.1016/j.engstruct.2019.109648

Ghandourah, E., Bendine, K., Khatir, S., Benaissa, B., Banoqitah, E., Alhawsawi, A. and Moustafa, E. (2023), "Novel approach-based sparsity for damage localization in functionally graded material", *Buildings*, **13**(7), 1768. https://doi.org/10.20944/preprints202307.0124.v1

Gong, C.X. and Zhang, Q. (2022), *Principles of Reliability Design for Engineering Structures*, China Machine Press, Beijing, China.

Ho, V., Khatir, S., De, R., Bui, T. and Abdel, W. (2020), "Finite element model updating of a cable-stayed bridge using metaheuristic algorithms combined with Morris method for sensitivity analysis", *Smart Struct. Syst., Int. J.*, **26**(4), 451-468. https://doi.org/10.12989/sss.2020.26.4.451

Jia, S., Han, B., Ji, W. and Xie, H. (2022), "Bayesian inference for predicting the long-term deflection of prestressed concrete bridges by on-site measurements", *Constr. Build. Mater.*, **320**, 126189. https://doi.org/10.1016/j.conbuildmat.2021.126189

Jorquera-Lucerga, J., Lozano-Galant, J. and Turmo, J. (2016), "Structural behavior of non-symmetrical steel cable-stayed bridges", *Steel Compos. Struct., Int. J.*, **20**(2), 447-468. https://doi.org/10.12989/scs.2016.20.2.447

Li, S., Zhu, S., Xu, Y., Chen, Z. and Li, H. (2012), "Long-term condition assessment of suspenders under traffic loads based on structural monitoring system: application to the Tsing Ma bridge", *Struct. Control Health Monitor.*, **19**, 82-101. https://doi.org/10.1002/stc.427

Li, X., Luo, H., Ding, P., Chen, X. and Tan, S. (2023), "Prediction study on the alignment of a steel-concrete composite beam track cable-stayed bridge", *Buildings*, **13**, 882. https://doi.org/10.3390/buildings13040882

Lu, Z., Wang, X., Zhao, B. and Ren, W. (2021), "Construction alignment prediction of large span waveform steel web continuous rigid bridge based on MEC-BP agent model", *J. Chang'an Univ.* (*Natural Science Edition*), **41**, 53-62. https://doi.org/10.19721/j.cnki.1671-8879.2021.06.006

Mei, D., Shan, D., Luo, L. and Gu, X. (2022), "Multivariate statistical sensitivity analysis of the completed structural state for long-span cable-stayed bridges", *Structures*, **41**, 51-65. https://doi.org/10.1016/j.istruc.2022.04.099

Mia, M. and Kameshwar, S. (2023), "Machine learning approach for predicting bridge components' condition ratings", *Front. Built Environ.*, **9**. https://doi.org/10.3389/fbuil.2023.1254269

Oulad Brahim, A., Capozucca, R., Khatir, S., Fahem, N., Benaissa, B. and Cuong-Le, T. (2024), "Optimal Prediction for Patch Design Using YUKI-RANDOM-FOREST in a Cracked Pipeline Repaired with CFRP", *Arab. J. Sci. Eng.*, **49**, 15085-15102. https://doi.org/10.1007/s13369-024-08777-1

Rageh, A., Eftekhar, A.Y. and Linzell D. (2019), "Steel railway bridge fatigue damage detection using numerical models and machine learning: mitigating influence of modeling uncertainty", *Int. J. Fatigue*, **134**, 105458. https://doi.org/10.1016/j.ijfatigue.2019.105458

Saadatmorad, M., Jafari-Talookolaei, R. and Khatir, S. (2024a), "Damage detection of beam-like structures using wavelet transform and subtraction of intact and damaged mode shapes", *HCMCOU J. Sci. – Adv. Computat. Struct.*, **2024**, 14-2. https://doi.org/10.46223/HCMCOUJS.acs.en.14.2.60.2024

Saadatmorad, M., Khatir, S., Abdushkour, H., Benaissa, B., Thobiani, F. and Khawaja, A. (2024b), "Structural Damage Detection by Derivative-Based Wavelet Transforms", *Res. Article-Mech. Eng.*, **49**, 15701-15709. https://doi.org/10.1007/s13369-024-09115-1

Saadatmorad, M., Khatir, S., thanh cuong, l., Benaissa, B.and Saïd, M. (2024c), "Detecting Damages in Metallic Beam Structures using a Novel Wavelet Selection Criterion", *J. Sound Vib.*, **578**, 118297. https://doi.org/10.1016/j.jsv.2024.118297

Seguini, M., Khatir, S., Boutchicha, D., Abdelmoumin, O., thanh cuong, l., Benaissa, B., Noori, M. and Fantuzzi, N. (2024), "Forecasting and characterization of composite pipeline based on experimental modal analysis and YUKI-gradient boosting", *Constr. Build. Mater.*, **425**. https://doi.org/10.1016/j.conbuildmat.2024.135625

Shan, D., Dong, H. and Gu, X. (2021), "Multivariate statistical sensitivity analysis for construction control of long-span cable-stayed bridges", *China J. Highway Transport*, (12), 68-79. https://doi.org/10.19721/j.cnki.1001-7372.2021.12.006

Su, C., Luo, X. and Yun, T. (2010), "Aerostatic reliability analysis of long-span bridges", *J. Bridge Eng.*, **15**, 260-268. https://doi.org/10.1061/(ASCE)BE.1943-5592.0000069

Tarhouni, I., Frómeta, D., Casellas, D., Costa, J. and Maimí, P. (2022), "Assessing the effect of the experimental parameters in the evaluation of the essential work of fracture in high-strength thin sheets", *Eng. Fract. Mech.*, **270**, 108560. https://doi.org/10.1016/j.engfracmech.2022.108560

TB 10092-2017 (2017), Code for Design of Concrete Structures of Railway Bridge and Culvert; Ministry of Transport of the People's Republic of China, Beijing, China.

TB 10127-2020 (2020), Code for Design of Concrete-filled Steel Tubular Structures of Railway Bridge, Ministry of Transport of the People's Republic of China, Beijing, China.

Tu, J., Liu, Y., Zhou, M. and Li, R. (2020), "Prediction and analysis of compressive strength of recycled aggregate thermal insulation concrete based on GA-BP optimization network", *J. Eng. Des. Technol.*, **19**, 412-422. https://doi.org/10.1108/JEDT-01-2020-0022

Tubaldi, E., Macorini, L. and Izzuddin, B.A. (2019), "Identification of critical mechanical parameters for advanced analysis of masonry arch bridges", *Struct. Infrastr. Eng.*, **16**, 328-345. https://doi.org/10.1080/15732479.2019.1655071

Wang, X., Chen, X., Yan, M. and Chang, M. (2018), "Constitutive model for ratcheting behavior of Z2CND18.12N austenitic stainless steel under non-symmetric cyclic stress based on BP neural network", *Steel Compos. Struct., Int. J.*, **28**(5), 517-525. https://doi.org/10.12989/scs.2018.28.5.517

Wang, Z., Zhang, W., Zhang, Y. and Liu, Z. (2023), "Temperature prediction of flat steel box girders of long-span bridges utilizing in situ environmental parameters and machine learning", *J. Bridge Eng.*, **27**(3). https://doi.org/10.1061/(ASCE)BE.1943-5592.0001840

Xin, J., Jiang, Y., Zhou, J., Peng, L., Liu, S. and Tang, Q. (2022), "Bridge deformation prediction based on SHM data using improved VMD and conditional KDE", *Eng. Struct.*, **261**, 114285. https://doi.org/10.1016/j.engstruct.2022.114285

Ye, D., Xu, Z. and Liu, Y. (2022), "Solution to the problem of bridge structure damage identification by a response surface method and an imperialist competitive algorithm", *Scientific Reports*, **12**(1). https://doi.org/10.1038/s41598-022-17457-9

Yi, T.H., Li H.N. and Sun, H.M. (2013), "Multi-stage structural damage diagnosis method based on energy-damage theory", *Smart Struct. Syst., Int. J.*, **12**(3), 345-361. https://doi.org/10.12989/sss.2013.12.3_4.345

Zhou, S., Deng, F., Han, Z., Yu, L. and Wu, L. (2019), "Construction alignment prediction for large-span continuous bridges based on optimal limit learning machine", *J. China Railway Soc.*, **41**, 134-140. https://doi.org/10.3969/j.issn.1001-8360.2019.03.018